A wavelength-selective photonic-crystal waveguide coupled to a nanowire light source

HONG-GYU PARK[1,2*†], CARL J. BARRELET[1*], YONGNING WU[1], BOZHI TIAN[1], FANG QIAN[1] AND CHARLES M. LIEBER[1,3]

[1]Department of Chemistry and Chemical Biology, Harvard University, Cambridge, Massachusetts 02138, USA
[2]Department of Physics, Korea University, Seoul 136-701, South Korea
[3]School of Engineering and Applied Sciences, Harvard University, Cambridge, Massachusetts 02138, USA
*These authors contributed equally to this work.
†e-mail: hgpark@korea.ac.kr

Published online: 7 September 2008; doi:10.1038/nphoton.2008.180

The efficient delivery of photons from light sources to photonic circuits is central to any fibre-optic or integrated optical system. Coupling light emitters to optical fibres or waveguides determines the photon flux available in, and therefore the performance of, photonic devices used in applications such as optical communication and information processing. Many solutions have been proposed to improve impedance matching in light-emitting diode-to-fibre or photonic-crystal cavity-to-waveguide systems; however, the efficient coupling of integrated light sources into nanophotonic circuits remains a challenge. Here, we propose an optically or electrically driven photonic structure that uses active semiconductor nanowires to light up photonic-crystal waveguides. The photonic crystal is used to either guide or filter out different colours of light as desired. In addition, we report an active nanowire-based optical structure that can generate two different colours of light and then send them in opposite directions. The hybrid nanowire/photonic-crystal waveguide represents a significant advance towards all-optical processing in nanoscale integrated photonic circuits and a new addition to the nanophotonic toolbox.

To develop all-optical processing in an ultra-compact photonic integrated system, nanophotonic devices are being pursued[1–10]. A semiconductor nanowire can act as a nanoscale light source with high radiance from its small emitting area and low power consumption[11,12]. Photonic-crystal waveguides have shown great potential for optical communication and optical computing[13,14]; however, efficient injection of light on a chip into the photonic-crystal waveguide remains a challenge[8–10]. Recently, different photonic building blocks have been brought together in hybrid photonic structures to combine different functionalities[15]. Hybrid photonic structures can offer viable solutions for the efficient injection of light on a chip into photonic-crystal waveguides. In this work, we investigate this hybrid photonic approach, which combines two state-of-the-art building blocks—active semiconductor nanowires and photonic-crystal waveguides.

RESULTS

OPTICALLY EXCITED NANOWIRES

Our hybrid structure consists of a CdS active semiconductor nanowire and a Si_3N_4 two-dimensional (2D) photonic-crystal freestanding slab waveguide (Fig. 1a). Si_3N_4 is a transparent material at $\lambda_c =$ 510 nm, the emission wavelength of CdS, with a refractive index of $\sim$2.1 (ref. 16). Single-crystal CdS nanowires with a typical diameter of $\sim$80 nm and a length of $\sim$5 μm are prepared by a metal-nanocluster-catalysed vapour–liquid–solid (VLS) growth process[17] and dispersed onto a Si_3N_4 film. To realize the structure of Fig. 1a, one first locates the exact position of nanowires with an optical microscope[15]. One then designs and lithographically fabricates the photonic-crystal waveguide around the nanowire (see Methods). This approach allows the fabrication of a hybrid structure that combines a direct bandgap nanostructure with a photonic crystal on a transparent dielectric slab. Such material combination on a single chip previously required advanced and complex fabrication procedures such as regrowth of a transparent material[9,10,18]. Our fabrication, on the other hand, is straightforward.

The 2D photonic-crystal structure is designed to overlap the electronic semiconductor bandgap of the CdS nanowire ($\sim$2.43 eV) with the guided mode of the photonic-crystal waveguide so as to inject light from the semiconductor band edge into the photonic-crystal waveguide. The structural parameters of the photonic crystal are optimized from the band structure of the straight single-line-defect waveguide calculated by a plane wave expansion simulation method[19] (Fig. 1b). For a lattice constant of 185 nm and a hole diameter of 92.5 nm, the photonic band structure overlaps the waveguide mode with the CdS emission energy in the photonic bandgap.

Figure 1c shows a scanning electron micrograph (SEM) of a fabricated nanowire photonic-crystal waveguide. A large hole is lithographically defined at the end of the waveguide into the Si_3N_4 substrate to provide a well-defined output scattering site. We measured the injection and guidance of light from the CdS nanowire into the photonic-crystal waveguide using a home-built epifluorescence microscope for optical excitation (see Methods).

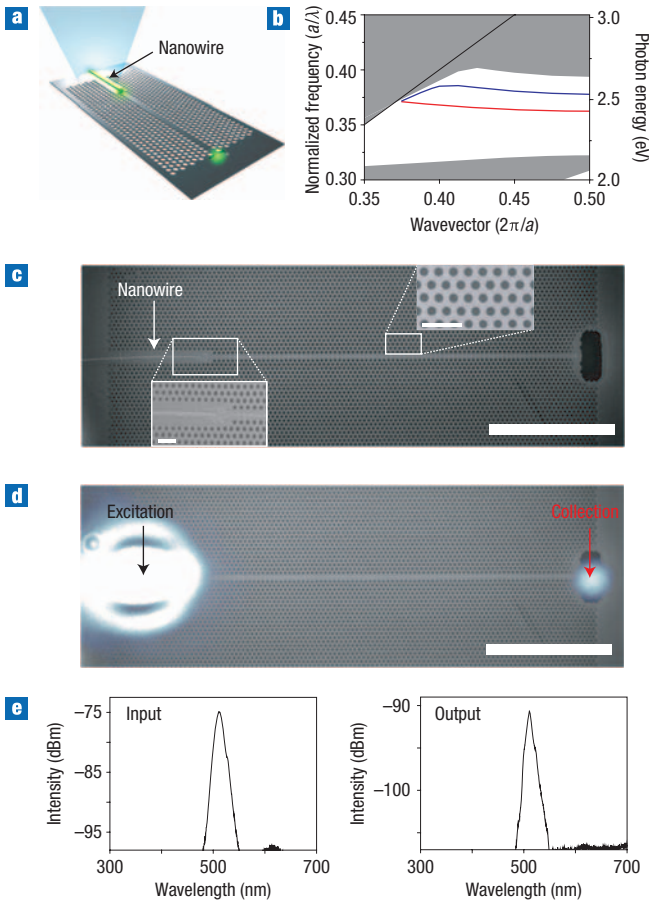

Figure 1 Optical injection from the CdS semiconductor nanowire into the photonic-crystal waveguide. a, Schematic of the 2D photonic bandgap structure made in a Si_3N_4 slab with the straight line-defect waveguide aligned with the CdS nanowire. **b**, Calculated TE-like band structure of the straight single-line-defect photonic-crystal waveguide. In simulation, the lattice constant *a*, the hole radius and the slab thickness are 185 nm, 0.25*a* and 1.08*a*, respectively. Even (red) and odd (blue) waveguide modes appear in the photonic bandgap (white region). Leaky modes (grey region) and light line (solid black line) are also shown. **c**, SEM of the CdS nanowire facing the straight waveguide terminated with a large hole used as an output scattering site and magnified SEM images of the nanowire (inset, left) and the photonic-crystal structure (inset, right). Inset scale bars, 500 nm. **d**, PL superimposed on the SEM image of **c**. Scale bars, 5 μm. **e**, PL spectra of the nanowire emission and the light scattered from the photonic-crystal waveguide output. The output power is measured at the spectrometer.

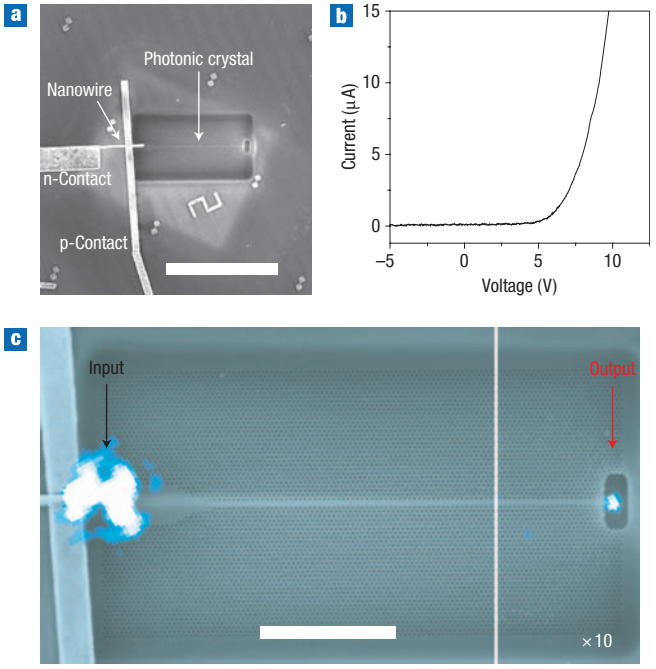

Figure 2 Light injection from an electrically driven nanowire LED structure into a photonic-crystal waveguide. a, SEM image of the entire nanowire LED device facing the photonic-crystal waveguide terminated with a large hole used as an output scattering site. Metal contacts are fabricated in the core/multishell nanowire LED. Scale bar, 20 μm. **b**, Current versus voltage data recorded from the nanowire LED. **c**, EL image superimposed on the SEM image. EL from the nanowire is efficiently guided by the photonic-crystal waveguide. Scale bar, 5 μm.

Photoluminescence (PL) of the nanowire was waveguided by both the photonic bandgap (horizontal direction) and total internal reflection (vertical direction)[18]. The PL image in Fig. 1d shows that light is rarely scattered in the middle of the waveguide because it propagates with low optical losses. In addition, the PL spectrum in Fig. 1e measured at the large hole (output) supports the efficient coupling from the nanowire into the waveguide. The PL spectrum of the CdS nanowire in the photonic-crystal waveguide is centred at ∼510 nm as expected[17]; however, the peak shape is different from the one in ref. 17 because of the presence of the photonic-crystal waveguide. The modification of the emission peak, because of the different transmission of the photonic-crystal waveguide at different wavelengths, has been observed previously in similar structures[4,10]. The successful demonstration of this hybrid structure using bottom-up and top-down approaches opens up a new possibility to simplify nanoscale integrated optical processing.

To investigate the device efficiency of the nanowire photonic-crystal waveguide, we used 3D finite-difference time-domain (FDTD) simulation[18,20]. We modelled the hybrid structure fabricated in Fig. 1c. The FDTD simulation shows that the probability of photons from the nanowire hitting the scattering target increases more than 100 times in our device compared with that in a freestanding nanowire surrounded by air. Direct injection of light emitted from the nanowire, which has a size comparable with that of the photonic crystal, into the waveguide leads to impedance matching in these two structures and thus increase in device efficiency. In addition, we estimated the experimental efficiency—defined as the transmission normalized by the injected power along the waveguide—to be >8% at 510 nm by analysing the measured PL spectra in Fig. 1e (see also Supplementary Information). Both the surface roughness of the waveguide and coupling between the nanowire and the photonic-crystal waveguide were considered for the estimation. The experimental efficiency of the hybrid structure is similar to that of a conventional semiconductor light-emitting diode (LED) coupled to a single-mode fibre[10]. Further optimization, such as adiabatic transformation[3] and non-uniform tapering[21,22] of the waveguide should allow a reduction of the optical losses generated at the interface of the two structures. A careful study of the surface roughness of the holes, which is the main reason for the waveguide loss[23], is necessary. In addition, the photonic-crystal structure can be improved to take full advantage of the Purcell effect[24] to enhance the spontaneous emission from the nanowire.

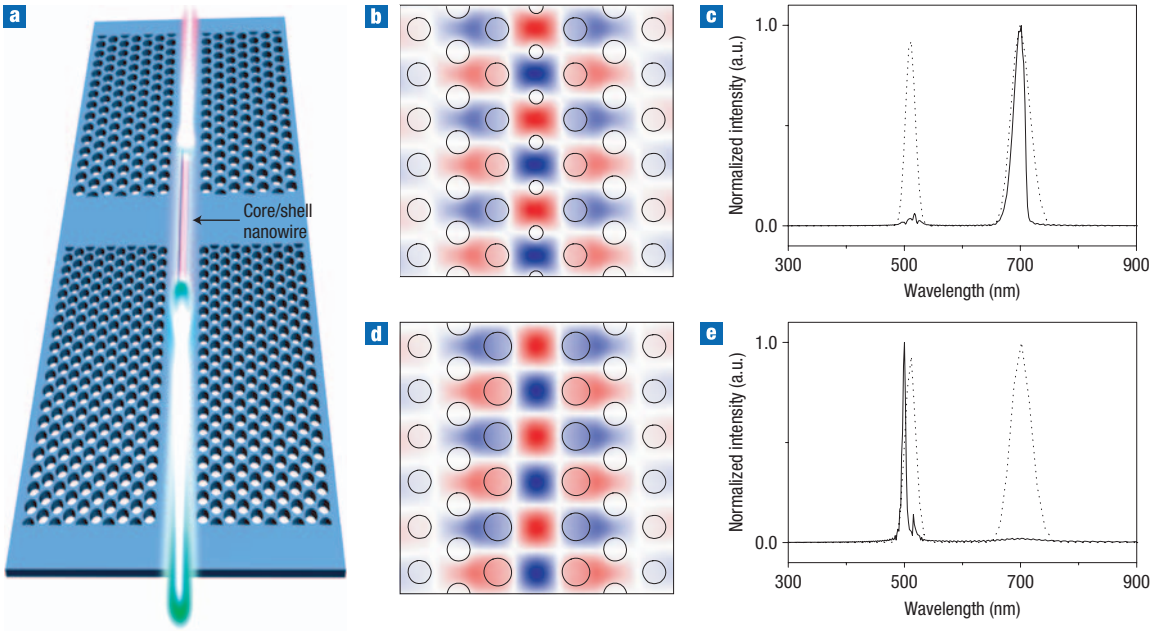

Figure 3 Characterization and modelling of the wavelength-selective nanowire/photonic-crystal structure. a, Schematic of the CdS/CdSe core/shell nanowire facing two different straight line-defect waveguides. The upper waveguide is designed to guide the red light and to filter out the green light, whereas the lower waveguide is designed to guide the green light and to filter out the red light. **b**, Schematic of the upper photonic-crystal waveguide and the calculated magnetic field of the TE-like waveguide mode superimposed on the waveguide. The lattice constant (a') is 280 nm. **c**, FDTD spectra of the TE-like waveguide mode for the upper waveguide (solid line) and a dipole source used to simulate the CdS and CdSe PL (dashed line). The distance between the dipole source and the output monitor is $34a'$. **d**, Schematic of the lower photonic-crystal waveguide and the calculated magnetic field of the TE-like waveguide mode superimposed on the waveguide. The lattice constant (a) is 185 nm. **e**, FDTD spectra of the TE-like waveguide mode for the lower waveguide (solid line) and the dipole source used to simulate the CdS and CdSe PL (dashed line). The distance between the dipole source and the output monitor is $34a$. The structural parameter d/d_0 is 1.2, where d and d_0 are the increased and the normal hole diameters, respectively.

ELECTRICALLY DRIVEN NANOWIRES

To explore the practical application of hybrid photonic structures, we fabricated an electrically driven device to light up the photonic-circuit waveguide on a chip. Electrical injection is a critical step for most practical applications of an integrated photonic system[12,18]. Semiconductor nanowires have been successfully used for efficient electroluminescence (EL) emission. Core/multishell radial nanowire heterostructures (n-GaN/i-InGaN/p-AlGaN/p-GaN) were synthesized by metal-organic chemical vapour using a strategy involving axial elongation by nanocluster-catalysed growth followed by controlled shell deposition onto the nanowire core[25]. As-synthesized nanowires were dispersed on a Si_3N_4 slab, and metal contacts deposited separately onto the p-type outer shell and n-type core at the ends of individual nanowires to inject holes and electrons simultaneously into the InGaN active medium, as previously described (Fig. 2a)[12]. The electrical characteristics of the nanowire LED are shown in Fig. 2b. This device in forward bias yields strong EL emission (with an external quantum efficiency up to $\sim$5.8%)[12] that is injected into the photonic-crystal waveguide. The photonic crystal was made using the same structural parameters as Fig. 1b because the emission spectrum of the InGaN nanowire ($\lambda_c = 480$ nm, 35 nm full-width at half-maximum) is similar to that of the CdS nanowire ($\lambda_c = 510$ nm, 16 nm full-width at half-maximum). EL from the nanowire is efficiently guided by the photonic-crystal waveguide, as shown in the EL image superimposed on the SEM image (Fig. 2c) and the typical EL spectrum (see Supplementary Information, Fig. S3). This result indicates that the electrically driven nanowire LED combined with the photonic-crystal waveguide provides, in practice, a highly directional light beam in the integrated photonic circuit.

WAVELENGTH-SELECTIVE OPERATION

To take full advantage of integrated photonic circuits, it would be desirable to operate with various colours of light emission. Here, we study a novel structure that generates two colours of light and separates them in two opposite directions on a chip. To generate multiple colours from a single nanowire, we take advantage of the bottom-up synthesis of core/shell nanowires consisting of two semiconductor materials[26], in which a CdS nanowire core emits green light and the CdSe shell emits red. To direct the two emitted colours in opposite directions, we define two photonic-crystal waveguides in each direction with different lattice constants[27]. In this nanoscale light source with wavelength-selective output ports, each colour of light has a preferred propagating direction.

Figure 3a shows a schematic of the wavelength-selective nanowire photonic structure consisting of a CdS/CdSe core/shell nanowire aligned with two straight line-defect photonic-crystal waveguides at either end. Using the semiconductor band edges of CdS and CdSe, the nanowire generates green and red photons. On the upper end of the nanowire, the photonic-crystal waveguide (Fig. 3b) is designed to specifically guide the red light and to filter out the green. The structural parameters are optimized to generate transverse electric (TE)-like photonic-crystal waveguide modes[20] for the red colour. To filter out the green light, small holes are introduced at the centre of the waveguide (with a diameter d). We have systematically studied the effect of the small holes on the attenuation (optical losses) of the green light. We noticed a pronounced attenuation of the green light as the hole size increases (see Supplementary Information, Fig. S2b). This behaviour is expected because green light is above the light line in the photonic band structure that prevents both TE-like and transverse magnetic

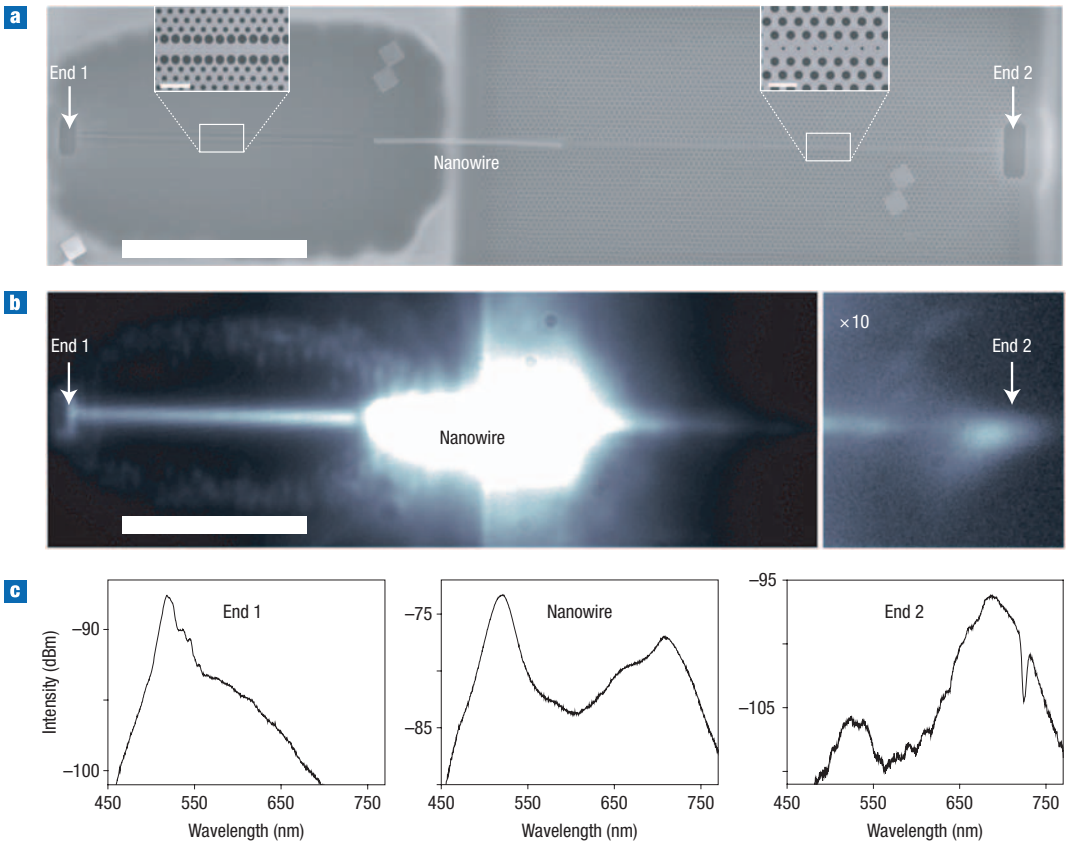

Figure 4 PL study of the wavelength-selective nanowire/photonic-crystal structure. a, SEM image of the nanoscale light source with wavelength-selective output ports composed of the CdS/CdSe core/shell nanowire aligned with two different straight line-defect waveguides terminated by output scattering sites. Scale bar, 10 μm. End 1 indicates the output scattering site of the photonic-crystal waveguide for the green light, and End 2 indicates the one for red light. Insets: Magnified SEM images of both photonic-crystal waveguides (scale bars of 500 nm). **b**, PL imaging of the nanowire photonic structure where light scatters out at the two waveguide outputs. Light scattered along the photonic-crystal waveguide indicates the attenuation of the desired colour. Scale bar, 10 μm. **c**, PL spectra from the nanowire and from both waveguide output scattering sites: End 1 and End 2. The output power is measured at the spectrometer.

(TM)-like green modes from being waveguided. Furthermore, we have carried out 3D FDTD simulation for this photonic-crystal waveguide structure with a structural parameter d/d_0 of 0.6 (where d_0 is the normal hole diameter). The results show that when two colours (two dipole sources) of equal intensities are injected into this waveguide, only red light propagates efficiently through the waveguide, with the green light being filtered out (Fig. 3c).

The photonic-crystal waveguide at the other end of the nanowire is designed to do the exact opposite: it guides the green light and filters out the red (Fig. 3d). The structural parameters and the photonic band structure are similar to the waveguide of Fig. 1b except for one modification: the nearest-neighbour holes (with a diameter d) around the waveguide have a larger diameter. We have studied the optical properties of this waveguide structure using the 3D FDTD method (see Methods). Simulation shows that when two colours (two dipole sources) of equal intensities are injected into the waveguide, only green light propagates efficiently through the waveguide, the red light being filtered out (Fig. 3e). We systematically studied the effect of nearest-neighbour holes around the waveguide on the attenuation of red light using the 3D FDTD method. The attenuation of red light increases markedly with increasing hole diameter d (see Supplementary Information, Fig. S2d). The green light lies in the photonic bandgap and therefore the photonic crystal guides it with low optical losses, but the red light, which is outside the photonic bandgap and guided by effective refractive index contrast[20], suffers large optical losses (see Methods). In summary, the 3D FDTD simulation supports that photonic-crystal waveguides can guide one colour, while filtering out the other. This results in a novel photonic structure capable of both generating two colours of light on a chip and separating them into two opposite directions.

In the SEM of the fabricated wavelength-selective active photonic structure (Fig. 4a), the CdS/CdSe core/shell nanowire is introduced at the centre of the structure. The nanowire was grown in two sequential steps using two different molecular precursors (see Methods). The magnified SEM images (insets in Fig. 4a) show the two photonic-crystal waveguides discussed in Fig. 3. Using the same fabrication procedure as in Fig. 1c, two photonic-crystal waveguides were defined at either end of the nanowire. The structural parameters, d/d_0, of left and right photonic-crystal waveguides are $\sim$1.5 and $\sim$0.4, respectively.

PL imaging shows that photons generated from the nanowire body are injected into the two photonic-crystal waveguides and scattered out of their large holes (Fig. 4b). In contrast to the PL imaging in Fig. 1d, light is scattered along the waveguides because of the attenuation of the desired colour. The output scattering sites labelled End 1 and End 2 show the light guided and exiting the photonic-crystal waveguides. To characterize the structure, we studied the optical properties using PL spectroscopy. The PL spectrum of the CdS/CdSe core/shell nanowire contains two peaks: one centred at $\sim$510 nm and the other at $\sim$700 nm (Fig. 4c, middle panel). The green and red

emissions correspond to the band edges of the CdS and CdSe bandgaps. The PL spectroscopy measurements of the light scattered from the large hole at each end of the waveguide show that the two specially designed photonic-crystal waveguides efficiently filter out a desired colour of light (Fig. 4c, left and right panels). The 3D FDTD spectrum shown in Fig. 3 supports the experimental measurements in which we generate two colours on a chip and split them into two opposite directions. The difference in relative losses of waveguided green and red colours at Ends 1 and 2 (Fig. 4c) is responsible for the different surface roughness of the holes on the two sides of the photonic-crystal waveguide. Further progress on the synthesis of the core/shell nanowire and fabrication of the photonic-crystal waveguide would allow improvement of the device performance. Our hybrid nanowire photonic structure will enable a significant advance in complexity and functionality of the building blocks for ultra-compact photonic nanocircuits.

DISCUSSION

In summary, state-of-the-art nanofabrication was performed to combine a bottom-up synthesized single-crystal semiconductor nanowire emitter with a top-down fabricated photonic-crystal waveguide. We measured the efficient injection and waveguiding of light from the optically or electrically driven active semiconductor nanowires into the 2D photonic-crystal Si_3N_4 freestanding slab waveguide. In addition, the nanoscale light source with wavelength-selective output ports was successfully demonstrated by showing that two colours of light emitted from the CdS/CdSe core/shell nanowire are split into two opposite directions. We believe that the rapid progress in developing this hybrid nanowire photonic-crystal waveguide represents an important step towards all-optical processing in nanoscale integrated photonic systems as well as encouraging practical applications of single-photon sources[18]. Furthermore, with the development of methods of nanowire assembly over a large area with controlled orientation and density[28], hybrid nanowire photonic-crystal systems will be more powerful building blocks in nanophotonics.

METHODS

FABRICATION OF THE PHOTONIC-CRYSTAL WAVEGUIDE

Synthesized active semiconductor nanowires were isolated as stable solution suspensions by sonication of the growth substrate in ethanol for 5–10 s and subsequently dispersed on a $Si_3N_4/SiO_2/Si$ wafer structure from the solution. The thicknesses of Si_3N_4 and SiO_2 were ~200 and 1,000 nm, respectively. A layer of 400-nm polymethyl methacrylate (PMMA) was deposited on the wafer, and electron-beam lithography with electron energy of 30 keV used to define a photonic-crystal structure. The PMMA layer also acted as a mask for the following reactive ion etching (RIE) process to drill air holes in the Si_3N_4 layer. RIE was operated using CF_4 and H_2 gases for 240 s at a total pressure of 10 mtorr and a power of 150 W. Wet etching of SiO_2 layer followed to make the Si_3N_4 layer a freestanding slab using buffered oxide etchant for 10 min.

SYNTHESIS OF THE CdS/CdSe CORE/SHELL NANOWIRE

The growth of a core/shell nanowire heterostructure was achieved by the following two steps. Single-crystal CdS nanowires were first grown by means of a catalyst-mediated VLS process using commercially available CdS powder and then the CdSe shells were deposited *in situ* by means of a homogeneous chemical vapour deposition process by thermal evaporation of CdSe (see Supplementary Information, Fig. S1). The synthesis temperature was tuned to avoid the formation of a CdSSe alloy at the interface of the CdS core and CdSe shell.

PL MEASUREMENT SETUP

The PL experiments were carried out by exciting the nanowires using frequency-doubled Ti:sapphire laser pulses with a wavelength of 400 nm. The light emitted from the individual nanowire were collected by a ×40 objective focused onto either a spectrometer or a silicon CCD camera that detects all visible colours.

3D FDTD SIMULATION SCHEME

The Si_3N_4 freestanding slab with a refractive index of 2.1 and a thickness of 200 nm was introduced in the calculation domain with a size of $40a \times 30a \times 6a$, where a is the lattice constant of the photonic-crystal structure. The computation grid size was one-tenth of the lattice constant. Dipole sources were introduced at one end of the photonic-crystal waveguide, and the waveguide modes measured at two detection planes located apart from the sources by a and $34a$. Attenuation values were computed by comparing total Poynting vectors at one detection plane with respect to the other plane (see Supplementary Information, Fig. S2). The size of the detection plane was $5.1a \times 600$ nm. In Fig. S2, only TE-like waveguide modes are considered. The same analysis can be applied to TM-like red light that is guided by the same mechanism as TE-like red light (see Supplementary Information, Fig. S2d). Similar attenuation values were computed for the TM-like red light as a function of increased hole diameter d.

Received 31 January 2008; accepted 30 July 2008; published 7 September 2008.

References

1. Coldren, L. A. & Corzine, S. W. *Diode Lasers and Photonic Integrated Circuits* (Wiley, New York, 1995).
2. Shani, Y., Henry, C. H., Kistler, R. C., Orlowsky, K. J. & Ackerman, D. A. Efficient coupling of a semiconductor-laser to an optical fiber by means of a tapered waveguide on silicon. *Appl. Phys. Lett.* **55,** 2389–2391 (1989).
3. Xu, Y., Lee, R. K. & Yariv, A. Adiabatic coupling between conventional dielectric waveguides and waveguides with discrete translational symmetry. *Opt. Lett.* **25,** 755–757 (2000).
4. Olivier, S. *et al.* Cascaded photonic crystal guides and cavities: spectral studies and their impact on integrated optics design. *IEEE J. Quantum Electron.* **38,** 816–824 (2002).
5. McNab, S. J., Moll, N. & Vlasov, Y. A. Ultra-low-loss photonic integrated circuit with membrane-type photonic crystal waveguides. *Opt. Express* **11,** 2927–2939 (2003).
6. Notomi, M., Shinya, A., Mitsugi, S., Kuramochi, E. & Ryu, H.-Y. Waveguides, resonators and their coupled elements in photonic crystal slabs. *Opt. Express* **12,** 1551–1561 (2004).
7. Noda, S., Chutinan, A. & Imada, M. Trapping and emission of photons by a single defect in a photonic bandgap structure. *Nature* **407,** 608–610 (2000).
8. Barclay, P. E., Srinivasan, K., Borselli, M. & Painter, O. Efficient input and output fiber coupling to a photonic crystal waveguide. *Opt. Lett.* **29,** 697–699 (2004).
9. Benisty, H., Lourtioz, J. M., Chelnokov, A., Combrie, S. & Checoury, X. Recent advances toward optical devices in semiconductor-based photonic crystals. *Proc. IEEE* **94,** 997–1023 (2006).
10. Yu, P. C., Topolancik, J., Chakravarty, S. & Bhattacharya, P. Mode-coupling characteristics and efficiency of quantum-dot electrically injected photonic crystal waveguide-coupled light-emitting diodes. *IEEE J. Quantum Electron.* **41,** 455–460 (2005).
11. Barrelet, C. J., Greytak, A. B. & Lieber, C. M. Nanowire photonic circuit elements. *Nano Lett.* **4,** 1981–1985 (2004).
12. Qian, F., Gradecak, S., Li, Y., Wen, C. Y. & Lieber, C. M. Core/multishell nanowire heterostructures as multicolor, high-efficiency light-emitting diodes. *Nano Lett.* **5,** 2287–2291 (2005).
13. Mekis, A. *et al.* High transmission through sharp bends in photonic crystal waveguides. *Phys. Rev. Lett.* **77,** 3787–3790 (1996).
14. Soljacic, M. & Joannopoulos, J. D. Enhancement of nonlinear effects using photonic crystals. *Nature Mater.* **3,** 211–219 (2004).
15. Barrelet, C. J. *et al.* Hybrid single-nanowire photonic crystal and microresonator structures. *Nano Lett.* **6,** 11–15 (2006).
16. Lide, D. R. (ed.). *CRC Handbook of Chemistry and Physics, Internet Version 2007*, 87th edn (Taylor & Francis, Boca Raton, FL, 2007).
17. Barrelet, C. J., Wu, Y., Bell, D. C. & Lieber C. M. Synthesis of CdS and ZnS nanowires using single-source molecular precursors. *J. Am. Chem. Soc.* **125,** 11498–11499 (2003).
18. Park, H.-G. *et al.* Electrically driven single-cell photonic crystal laser. *Science* **305,** 1444–1447 (2004).
19. Johnson, S. G., Fan, S. H., Villeneuve, P. R., Joannopoulos, J. D. & Kolodziejski, L. A. Guided modes in photonic crystal slabs. *Phys. Rev. B* **60,** 5751–5758 (1999).
20. Loncar, M., Vuckovic, J. & Scherer, A. Methods for controlling positions of guided modes of photonic-crystal waveguides. *J. Opt. Soc. Am. B* **18,** 1362–1368 (2001).
21. Ayre, M., Karle, T. J., Wu, L. J., Davies, T. & Krauss, T. F. Experimental verification of numerically optimized photonic crystal injector, Y-splitter, and bend. *IEEE J. Sel. Areas Commun.* **23,** 1390–1395 (2005).
22. Khoo, E. H., Liu, A. Q. & Wu, J. H. Nonuniform photonic crystal taper for high-efficiency mode coupling. *Opt. Express* **13,** 7748–7759 (2005).
23. Baba, T., Iwai, T., Fukaya, N., Watanabe, Y. & Sakai, A. Light propagation characteristics of straight single-line-defect waveguides in photonic crystal slabs fabricated into a silicon-on-insulator substrate. *IEEE J. Quantum Electron.* **38,** 743–752 (2002).
24. Vahala, K. J. Optical microcavities. *Nature* **424,** 839–846 (2003).
25. Qian, F. *et al.* Gallium-nitride-based nanowire radial heterostructures for nanophotonics. *Nano Lett.* **4,** 1975–1979 (2004).
26. Lauhon, L. J., Gudiksen, M. S., Wang, D. & Lieber, C. M. Epitaxial core-shell and core-multishell nanowire heterostructures. *Nature* **420,** 57–61 (2002).
27. Song, B. S., Noda, S. & Asano, T. Photonic devices based on in-plane hetero photonic crystals. *Science* **300,** 1537 (2003).
28. Yu, G., Cao, A. & Lieber, C. M. Large-area blown bubble films of aligned nanowires and carbon nanotubes. *Nature Nanotech.* **2,** 372–377 (2007).

Supplementary Information accompanies this paper at www.nature.com/naturephotonics.

Acknowledgements

We thank J. K. Yang, M. K. Seo, S. H. Kwon and Y. H. Lee for help with FDTD simulation and W. I. Park for help with fabrication. This work was supported by the Air Force Office of Scientific Research. H.G.P. acknowledged the support of this work by OPERA of the KOSEF and the Seoul R & BD Program.

Author information

Reprints and permission information is available online at http://npg.nature.com/reprintsandpermissions/.
Correspondence and requests for materials should be addressed to H.-G. P.